J|A|C|S
COMMUNICATIONS

Published on Web 06/24/2008

Electrogenerated Chemiluminescence of Single Conjugated Polymer Nanoparticles

Ya-Lan Chang, Rodrigo E. Palacios, Fu-Ren F. Fan, Allen J. Bard, and Paul F. Barbara*

Department of Chemistry and Biochemistry, Center for Nano- and Molecular Science and Technology and Center for Electrochemistry, The University of Texas at Austin, Austin, Texas 78712

Received May 9, 2008; E-mail: p.barbara@mail.utexas.edu

We describe the measurement of the electrogenerated chemiluminescence (ECL)[1] of single immobilized nanoparticles (NPs) based on the recently developed single molecule spectroelectrochemistry (SMS-EC)[2] technique. While ECL research on NPs has focused on the properties of particle ensembles,[3–6] the exploration of ECL at the single particle level reported herein allows for the investigation of effects due to particle heterogeneity, which are masked in bulk ECL and EC studies of NPs. Moreover, because ECL involves the generation of light electrochemically, the background signal is very low and thus it can provide the basis of a highly sensitive single particle electroanalytical method. We use this new approach to study ECL of NPs ($r = 25 \pm 15$ nm) of a conjugate polymer, such as poly(9,9-dioctylfluorene-*co*-benzothiadiazole) (F8BT, Figure 1a), widely used in solar cells and OLEDs.[7]

Our approach is based on rapid EC reactions of F8BT NPs immobilized at ITO working electrode (WE) in an electrochemical cell (Figure 1b) with a gold counter electrode (CE) and a silver quasi-reference electrode (QRE). The cells were filled with an acetonitrile solution containing 0.1 M $LiClO_4$ (supporting electrolyte) and a co-reactant (tri-*n*-propylamine, TPrAH[8]). In typical experiments, the potential of the working electrode (vs QRE) of a pristine cell was pulsed or linearly scanned (between 0 and 1.8 V) while simultaneously measuring the total cell current and the ECL intensity, I_{ECL}, of individual F8BT NPs as a function of potential. During this step, both the F8BT NP and the TPrAH are oxidized, the F8BT$\bullet^+$ is probably transported by hole-hopping along the surface of the NP, and the reaction between F8BT$\bullet^+$ and TPrA$\bullet$ produces the excited state in the polymer NP (see Supporting Information). Figure 1c,d shows the ECL and photoluminescence (PL) images of individual immobilized NPs. The inset in Figure 1c shows ECL spots due to four individual NPs with virtually no detectible background noise (on average $\ll$1 photoelectron per pixel).

Figure 2a shows ensemble averages of the luminescence intensity (PL + ECL) of ~94 NPs as a function of potential for a sample under laser excitation (8 mW/cm^2). Without TPrAH (see red curve of Figure 2a), the total luminescence intensity drops dramatically at potentials positive of ~1.1 V due to luminescence quenching by the injected holes and irreversible oxidation of F8BT, as seen previously.[2] On the other hand, when TPrAH is present, the PL quenching in the 1.1−1.6 V region was significantly reduced, presumably due to neutralization of holes at the particle surface via electron transfer by both TPrAH and TPrA radical (TPrA$\bullet$) (see reaction scheme in Supporting Information). Beyond 1.6 V, the total luminescence intensity increased sharply due to the contribution from ECL, which has comparable intensity to PL as the potential reached 1.8 V. Figure 2b (black curve) shows the ensemble average luminescence intensity of NPs located at the edge of image in Figure 1d where the laser excitation power (and as a result the PL) is negligible. Note that the irreversible electrochemical oxidation of F8BT is also suppressed by TPrA$\bullet$ reacting with the F8BT radical cations, thus promoting better reversibility of the F8BT oxidation process in the presence of TPrAH.

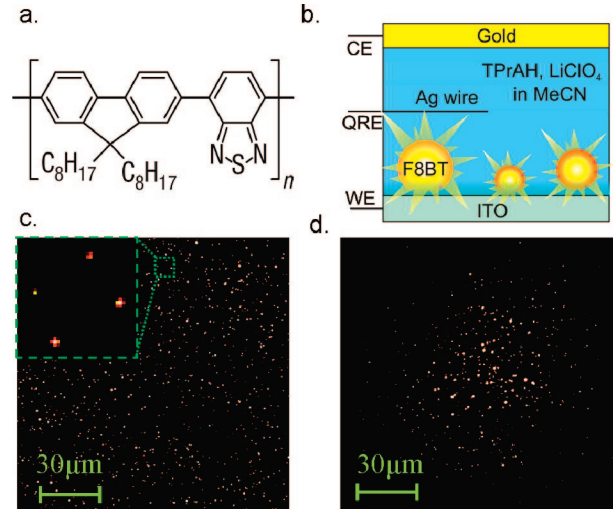

Figure 1. (a) F8BT chemical structure. (b) Schematic diagram of SMS-EC cell. (c) Wide-field ECL image. (d) Wide-field PL image (same area as c) with the laser beam focused on the central area of the image (inset: expanded region showing ECL from four particles). The intensity scale (0−200 counts) and integration time (0.5 s) of images c and d are the same.

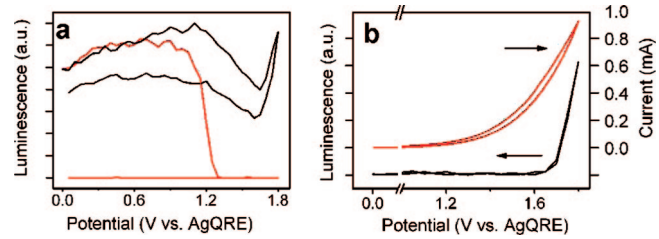

Figure 2. (a) Ensemble average of normalized (at potential = 0 V) single NPs' luminescence intensity trajectories under laser excitation with (black curve, 94 NPs) and without (red curve, 123 NPs) TPrAH. Data were acquired with a bias scan rate of 0.1 V/s. (b) Ensemble average of single NPs' ECL intensity trajectories (black curve) outside of laser spot with 0.1 M TPrAH (same cycle as black curve in a) and its corresponding voltammogram (red curve).

Figure3a portrays the ensemble averaged ECL intensity trajectories for 136 NPs recorded with a potential pulsed step from 0 to 1.5 V with no laser excitation. Three individual trajectories from the ensemble are shown in Figure 3c−e. Particle-to-particle variation in the maximum ECL photon flux (at ~40 s) is shown in the inset of Figure 3a. This broad distribution is primarily due particle-to-particle size variations, not variations in the ECL efficiency, as evidenced by the observation of a strong correlation

10.1021/ja803454x CCC: $40.75

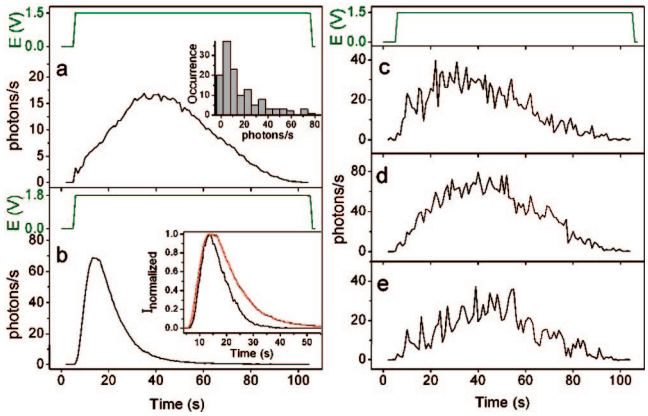

Figure 3. (a) Ensemble average of single NP ECL intensity trajectories (131 NPs) in a pristine cell without laser excitation. The green curve shows the applied bias. Inset: Histogram of maximum ECL photon flux for individual NPs for the data in panel a. (b) Same as panel a using different bias, 860 NPs. Inset: normalized subensembles constructed by sorting the particles based on the intensity at the maximum of their ECL time trajectories. The red curve is an average of the normalized ECL time trajectories of the 430 most intense NPs, the remaining NPs were averaged to give the black curve. (c,d,e) Examples of individual trajectories of single NPs corresponding to the data shown in a.

of single particle ECL and PL intensities (see Supporting Information). Here PL was recorded prior to the voltage step using a short light pulse and is an indirect measure of particle size. Unlike previously reported conventional ECL on bulk conjugated polymer films (e.g., MEH-PPV),[9] a long build-up time between voltage application and maximum photon flux was observed in the single NP experiments (~35 s for an ensemble of single F8BT NPs with a 0−1.5 V pulsed bias in a pristine SMS-EC cell, Figure 3a). Individual ECL trajectories (Figure 3c−e) demonstrate that the build-up time is similar for different NPs in the ensemble.

Figure 3a,b demonstrates the bias effect on the kinetics of ECL (i.e., build-up and decay time). ECL build-up and decay times decreased with a higher applied bias on pristine SMS-EC cells. The ECL peak photon flux is larger at more positive bias consistent with the greater rates of TPrAH and F8BT oxidation. In fact, at the lower biases (<1.5 V), it is difficult to observe ECL with an adequate signal-to-noise due to the lower ECL fluxes and longer ECL build-up times despite appreciable current from TPrAH oxidation at above ~1.1 V.

This build-up time might be related to the EC "break in"[10] phenomena related to penetration of solvent and ions that is ubiquitously observed in polymer films. Our results indicate that break in is associated with a nanoscopic rather than a mesoscopic structural/morphological change in the material, which is absent in the NP samples. This is supported by the observation that while NP ECL dynamics are only slightly heterogeneous the ECL dynamics for bulk F8BT thin films (~15 nm) reveal order of magnitude variations in the ECL rise and decay times as a function of sample position on the 10−100 s time scales (data not shown). Additionally, the ECL build-up time could be related to the slow mobility of large counteranions (ClO_4^-) in the polymer. Preliminary control experiments in oxygen-depleted conditions suggest that the ECL buildup is not primarily due to the presence of oxygen (see Supporting Information). However, more rigorous experiments are needed to confirm this point. The observed ECL decay time is probably related to some irreversible decomposition of $F8BT^{\bullet+}$ that competes with the reaction with the co-reactant. Depletion of TPrAH is probably not responsible for the decay since TPrAH concentration was high (0.1 M) and the currents were well below those for diffusion-limited TPrAH oxidation (see red curve of Figure 2c). Subensemble intensity trajectories for smaller (less intense ECL) and larger (more intense ECL) particles (inset in Figure 3b) reveal a longer decay time for larger particles for unknown reasons.

In conclusion, we have demonstrated a powerful method of observing ECL from single immobilized nanoparticles (NPs). To the best of our knowledge, this is the first report of ECL from sub-25 nm single NPs. In comparison to other optical, conductivity, and mass signals using nanoparticles,[11] the catalytic ECL amplification by co-reactant should allow study of the dynamics of the process and information about the heterogeneous electron-transfer kinetics at the single particle level. Thus, in addition to the usual advantage of single particle studies compared to ensembles of obtaining information about particle environments, this approach may also provide dynamic information not seen in ensembles. Moreover, because of high sensitivity, low background, and high spatial and potentially high temporal resolution of ECL, it should be useful as a very sensitive analytical method.

Acknowledgment. This work was supported by the National Science Foundation, the Department of Energy, BES, and the Welch Foundation.

Supporting Information Available: Details on materials, experimental procedures, reaction schemes, CV of thin film, and oxygen effect experiments. This material is available free of charge via the Internet at http://pubs.acs.org.

References

(1) Bard, A. J., Ed. *Electrogenerated Chemiluminescence*; Marcel Dekker: New York, 2004.
(2) (a) Palacios, R. E.; Fan, F.-R. F.; Bard, A. J.; Barbara, P. F. *J. Am. Chem. Soc.* **2006**, *128*, 9028. (b) Palacios, R. E.; Fan, F.-R. F.; Grey, J. K.; Suk, J.; Bard, A. J.; Barbara, P. F. *Nat. Mater.* **2007**, *6*, 680.
(3) Bard, A. J.; Ding, Z.; Myung, N. *Struct. Bonding (Berlin)* **2005**, *118*, 1.
(4) Chen, M.; Pan, L.; Huang, Z.; Cao, J.; Zheng, Y.; Zhang, H. *Mater. Chem. Phys.* **2007**, *101*, 317.
(5) Shen, L.; Cui, X.; Qi, H.; Zhang, C. *J. Phys. Chem. C* **2007**, *111*, 8172.
(6) Guyot-Sionnest, P.; Wang, C. *J. Phys. Chem. B* **2003**, *107*, 7355.
(7) See for example: (a) Anderson, N. A.; Lian, T. Q. *Annu. Rev. Phys. Chem.* **2005**, *56*, 491. (b) Friend, R. H.; Gymer, R. W.; Holmes, A. B.; Burroughes, J. H.; Marks, R. N.; Taliani, C.; Bradley, D. D. C.; Dos Santos, D. A.; Bredas, J. L.; Logdlund, M.; Salaneck, W. R. *Nature* **1999**, *397*, 121. (c) Zhu, X. Y. *J. Phys. Chem. B* **2004**, *108*, 8778.
(8) Nofsinger, J. B.; Danielson, N. D. *Anal. Chem.* **1987**, *59*, 865. Miao, W.; Choi, J.-P. In *Electrogenerated Chemiluminescence*; Bard, A. J., Ed.; Marcel Dekker: New York, 2004; Chapter 5.
(9) (a) Richter, M. M.; Fan, F-R. F.; Klavetter, F.; Heeger, A. J.; Bard, A. J. *Chem. Phys. Lett.* **1994**, *226*, 115. (b) Janakiraman, U.; Dini, D.; Preusser, A.; Holmes, A. B.; Martin, R. E.; Doblhofer, K. *Synth. Met.* **2001**, *121*, 1685.
(10) Inzelt, G. In *Electroanalytical Chemistry*; Bard, A. J., Ed.; Marcel Dekker: New York, 1994; Vol. 18, pp 89−241 and refs cited therein.
(11) See for example: (a) Sonnichsen, C.; Reinhard, B. M.; Liphardt, J.; Alivisatos, P. A. *Nat. Biotechnol.* **2005**, *23*, 741. (b) Zhang, Z. L.; Pang, D. W.; Yuan, H.; Cai, R. X.; Abruna, H. *Anal. Bioanal. Chem.* **2005**, *381*, 833.

JA803454X